water

MDPI

Article

Integration of Wave Power Farms into Power Systems of the Adriatic Islands: Technical Possibilities and Cross-Cutting Aspects

Damir Šljivac [1,*], Irina Temiz [2], Branka Nakomčić-Smaragdakis [3] and Matej Žnidarec [1,*]

[1] Department for Power Engineering, Faculty of Electrical Engineering, Computer Science and Information Technology, Josip Juraj Strossmayer University of Osijek, Kneza Trpimira 2b, 31000 Osijek, Croatia
[2] Department of Electrical Engineering, Uppsala University, Box 65, 75103 Uppsala, Sweden; irina.temiz@angstrom.uu.se
[3] Faculty of Technical Sciences, University of Novi Sad, Trg D. Obradovica 6, 21000 Novi Sad, Serbia; nakomcic@uns.ac.rs
* Correspondence: damir.sljivac@ferit.hr (D.Š.); matej.znidarec@ferit.hr (M.Ž.)

Abstract: Wave energy is of interest for regions with high wave power potential, as well as for regions with modest wave power potential such as the Adriatic/Mediterranean coastlines and islands. In the present paper, the possibility of integrating a wave power farm with the power system of an island in the Adriatic Sea, combining the wave power with a battery energy storage system (BESS) and solar photovoltaics (PVs) is explored and its impact on the local weak low voltage grid is investigated. The load profile is typical of the demand (consumption) of an Adriatic island, in which the demand substantially increases during summer (the tourist season). The wave power technology is a point-absorbing wave energy converter (WEC) with a direct drive linear permanent-magnet synchronous generator power take-off device. Wave power farms (WPFs) consist of two to ten WECs. In this study, we show that the integration of a WPF consisting of two WECs into the grid is optimal and helps to reach zero grid exchange, and a BESS reduces the intermittency of the power flow into the grid. Since a potential wave power farm is to be installed in a populated recreational area, the technical study is complemented by discussion on cross-cutting aspects such as its environmental and social impact.

Keywords: wave power; wave energy converters; power system integration; cross-cutting aspects; Adriatic islands

Citation: Šljivac, D.; Temiz, I.; Nakomčić-Smaragdakis, B.; Žnidarec, M. Integration of Wave Power Farms into Power Systems of the Adriatic Islands: Technical Possibilities and Cross-Cutting Aspects. *Water* **2021**, *13*, 13. https://dx.doi.org/10.3390/w13010013

Received: 7 November 2020
Accepted: 18 December 2020
Published: 24 December 2020

1. Introduction

To tackle the problem of global warming, low carbon energy policies have stimulated the widespread installation of commercial solar photovoltaics (PVs) and wind power parks globally and in Europe [1,2]. However, the integration of renewable energy sources (RES) to the grid imposes another challenge—grid stability. An appropriate mix of RES distributed generation (DG) chosen for the site of interest can help to overcome this and to support the net load variability with a large share of RES DG [3]. Ocean and particularly wave energy is considered to be a promising and attractive energy source due to its relatively small short-term fluctuations [4] and high power density [5], yet it still remains untapped. Wave energy is also attractive since the wave power potential in some regions follows the seasonality of electrical energy demand [6,7]. The estimated wave energy potential has gone from 17 TWh/year in 2007 [8] to 92 PWh/year in 2016 [9], available at coastal areas, where about 50 percent of the world's population lives. The global wave power potential is shown in Figure 1.

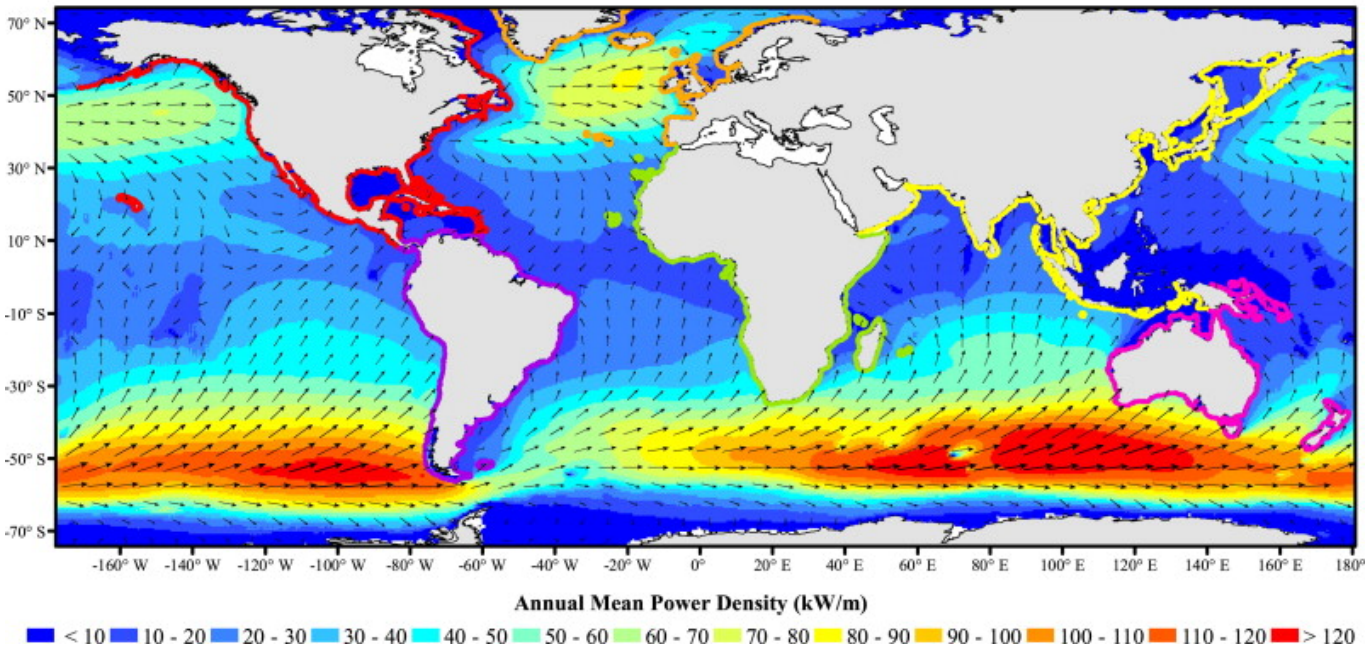

Figure 1. Global wave power potential. Reproduced with permission from [10].

Although the focus of many researchers and wave energy technology developers has been on areas with high wave power potential, even areas with relatively low potential have received attention. For example, the wave power potential has been studied for such regions as the Italian [11], Lithuanian [12] and Swedish [7] coastlines, in the Caspian Sea [13] and the Red Sea [14], offshore Mediterranean areas [15,16], as well as seas in China [17] and the Maldives [18]. The wave power density for these locations is given in Table 1. In this paper, the Adriatic Sea is of particular interest.

Table 1. Wave power density in different areas.

Geographical Region	Mean Wave Power Density * [kW/m]
Italian coastline [11]	1.7–4.3
Lithuanian coastline [12]	less than 2.4
Swedish coastline [7]	2.1–5.3
The Red Sea [14]	less than 3
The Mediterranean Sea, Malta [16]	less than 6.5
Maldives [18]	8.46–12.75
Caspian Sea [13]	5–14
China's coastal area [17]	6–16

* A range of values of wave power density is given when an estimate is made for several locations in the region.

This paper evaluates the possibility of integrating a wave power farm with the power system of an island in the Adriatic Sea, combining the wave power with a battery energy storage system (BESS) and solar photovoltaics (PVs), and its impact on the local weak low voltage grid. The wave power technology is a point-absorbing wave energy converter (WEC) with a direct drive linear permanent-magnet synchronous generator power take-off device, and is presented in Section 2. Wave power farms (WPFs) consist of two to ten WECs. The main idea of the case studies carried out and presented in Section 3 was to give a comprehensive analysis of various renewable electricity generation technologies that can be utilized together with a WPF to provide an electricity supply to meet the typical Adriatic island demand (consumption) throughout the entire year. The load profile used represents the typical demand (consumption) of an Adriatic island, in which the demand substantially increases during summer (the tourist season). Because of the large solar energy potential of this region, it is expected that PV systems will be integrated into this

power system; therefore, another case involving the simultaneous operation of a WPF and PV system is evaluated. Furthermore, the benefits of a BESS, together with a WPF and PVs, in achieving net zero electricity exchange with the grid is evaluated. Finally, Section 4 deals with economic, environmental and social aspects of WPFs.

2. Models and Methodology

2.1. Wave Power Potential and Wave Climate in the Adriatic Sea

The Republic of Croatia has 78 islands with a surface greater than 1 km^2 (44 islands inhabited by more than 15 people, 35 islands inhabited by more than 100 people, 17 islands inhabited by more than 1000 people), 525 small islands with surface between 0.1–1 km^2 and 389 small rock islands with a surface smaller than 0.1 km^2, which offers a great opportunity to integrate wave energy into the electric grid [19]. Wave power potential was assessed for the Adriatic Sea along the Croatian coastline in [20–22]. The mean wave power density is 1.96–2.68 kW/m, which is relatively low but can still be of interest for local islandic communities.

The wave power density P is calculated per unit length of the wave crest [23]:

$$P = \frac{\rho g}{64\pi} H_S^2 T_e \tag{1}$$

where ρ is the sea water density, g is the gravitational acceleration, H_S is the significant wave height and T_e is the wave energy period. A combination of H_S and T_e represents a sea state that is considered to be the same for at least 20–30 min. The significant wave height and energy period can be obtained from the wave power spectrum $S(\omega)$ via spectral moments m_n

$$m_n = \int_0^\infty S(\omega)\omega^n d\omega \tag{2}$$

where ω is the angular wave frequency. The significant wave height is given by

$$H_S = 4\sqrt{m_0} \tag{3}$$

and the wave energy period is given by

$$T_e = \frac{m_{-1}}{m_0} \tag{4}$$

In [21], the assessment of wave power potential was made for seven locations (see Figure 2) based on the World Wave Atlas (WWA), and the annual average energy yield was calculated for two wave energy converters, namely, for Pelamis and Aqua Buoy. Coordinates, water depth, wave climate and extreme values of significant wave height for return periods of 10 and 100 years for the selected locations are given in Tables 2 and 3. The water depth is determined based on bathymetry data (https://www.gebco.net/ (accessed on 24 October 2020). The wave spectrum of the Adriatic Sea is given in the form of a one-parameter modified JONSWAP wave spectrum [24]:

$$S(\omega) = 0.8626\frac{5}{16}\frac{H_S^2\omega^4}{\omega^5}\exp\left[-\frac{5}{4}\left(\frac{\omega_m}{\omega}\right)^4\right]1.78^p \tag{5}$$

where $p = \exp\left[-\frac{(\omega-\omega_m)^2}{2\sigma^2\omega_m^2}\right]$, $\omega_m = 0.52 + \frac{1.4}{H_S+0.7}$ is the modal frequency and $\sigma = 0.06$ if $\omega \leq \omega_m$ and $\sigma = 0.08$ if $\omega > \omega_m$.

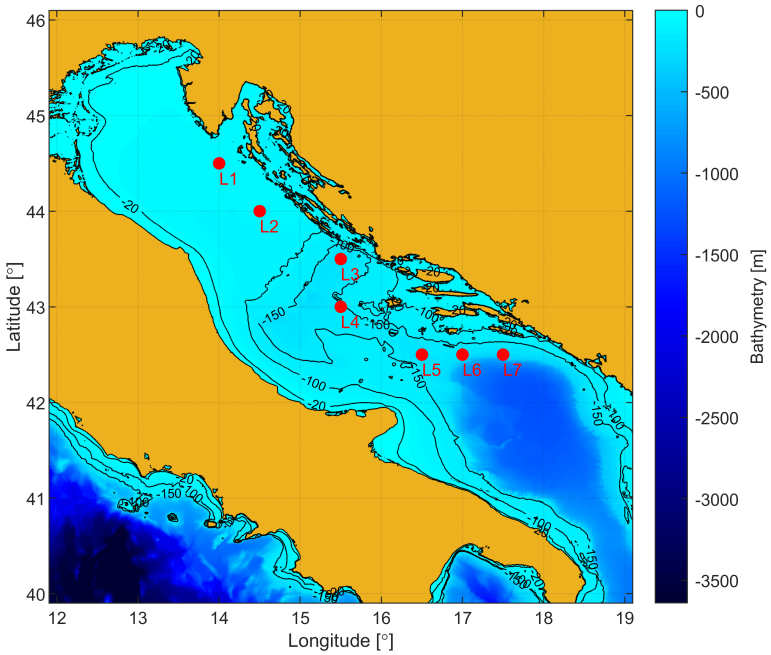

Figure 2. Seven locations along the Croatian coastline.

Table 2. Geographical coordinates of the selected locations in the Adriatic Sea and water depth. Reproduced with permission from [21].

Location	Latitude	Longitude	Water Depth (m)
L1	44.5° N	14.0° E	44
L2	44.0° N	14.5° E	72
L3	43.5° N	15.5° E	200
L4	43.0° N	15.5° E	172
L5	42.5° N	16.5° E	199
L6	42.5° N	17.0° E	193
L7	42.5° N	17.5° E	271

Table 3. Wave climate of the selected locations for two seasons: winter and summer. Reproduced with permission from [21].

Location	$H_{S,mean}$ (m)		$T_{e,mean}$ (s)		Extreme Values of H_S	
	Summer	Winter	Summer	Winter	$H_S(10)$ (m)	$H_S(100)$ (m)
L1	0.55	0.90	3.32	3.74	5.86	7.25
L2	0.55	0.93	3.28	3.79	6.07	7.51
L3	0.55	0.93	3.29	3.86	5.53	6.76
L4	0.58	1.00	3.69	4.53	5.68	6.93
L5	0.63	1.09	3.40	4.16	6.09	7.42
L6	0.61	1.07	3.37	4.15	6.26	7.66
L7	0.59	1.04	3.37	4.18	6.51	8.04

Wave power is converted to useful electrical power by means of wave energy converters (WECs). The first patent on a wave energy converter was registered in 1799 (Girard and Son, France) [25]. A new era for wave energy area started in the second half of the 20th century. The first commercial WECs were used in observation buoys in Japan and later in the USA from 1965 [26]. Since then, many different technologies for WECs have been proposed and these are classified based on different principles such as the location

of the WEC, its operational principles and its size with respect to the wave length and wave crest [27]. Based on the location, WECs can be classified as onshore, nearshore and offshore. Based on the operational principle, WECs are divided into oscillating water columns (OWCs), overtopping WECs and wave activated bodies (WABs), and the latter can be further divided based on the operational mode of the WEC: primarily pitching, surging and heaving devices. Based on the size with respect to the wave length, WECs are classified as attenuators, terminators and point absorbers. Some examples of WECs with their types are shown in Figure 3.

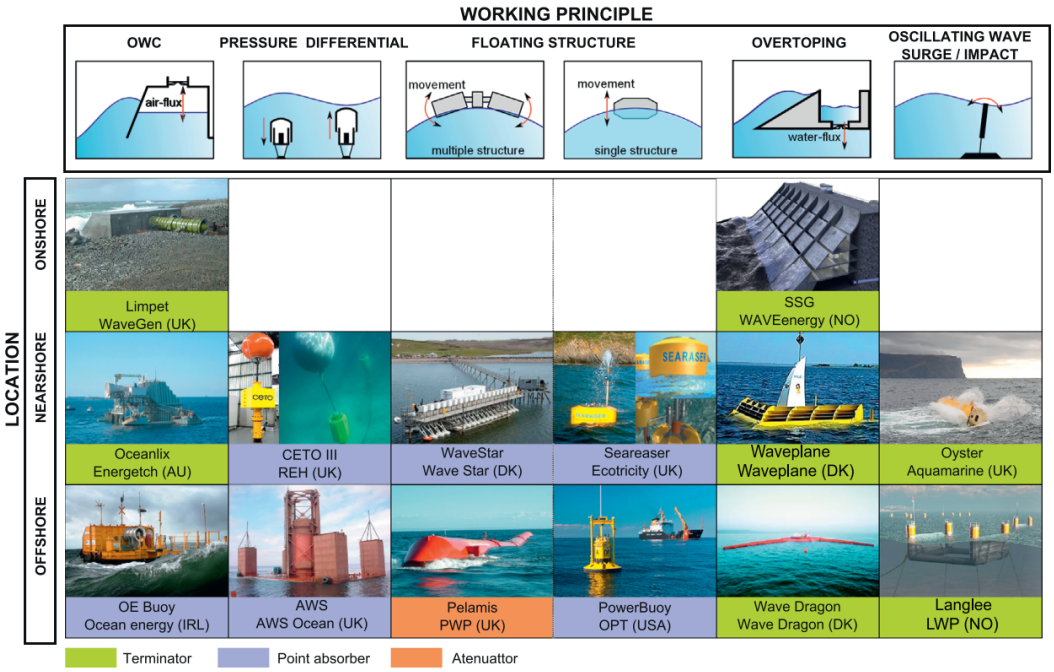

Figure 3. A classification of wave energy converters (WECs). Reproduced with permission from [5].

2.2. Wave Energy Conversion Technology from Uppsala University

The wave energy project at the Division of Electricity of Uppsala University (UU) started in 2002 and its first WEC was deployed in 2006. The concept developed at Uppsala University is a point-absorbing WEC, operating primarily in heave mode [28]. It consists of a floater placed on the water surface that is connected via a steel wire rope to a direct drive linear permanent-magnet generator (LPMG), see Figure 5. When the buoy moves, driven by waves, a translator mounted with permanent magnets moves inside the LPMG. Thus, an electromagnetic field (EMF) is induced in the stator coils due to their varying magnetic flux. The terminal voltages of the LPMG vary in amplitude and frequency (Figure 4) because of the reciprocal motion of the translator and irregular incoming waves. Therefore, power conversion is required.

One WEC has a limited power capacity, therefore several devices must be connected into a wave power farm (WPF) to deliver the required amount of power. Moreover, the aggregation effect is observed with an increased number of WECs in a WPF [29]. For UU's WEC, the electric power is collected in a marine substation where the three-phase current from each WEC is first rectified and fed to a common DC bus, then inverted to a three-phase AC current to be further connected to the grid. Additional electric components can be added to the marine substation to ensure power quality for grid connection.

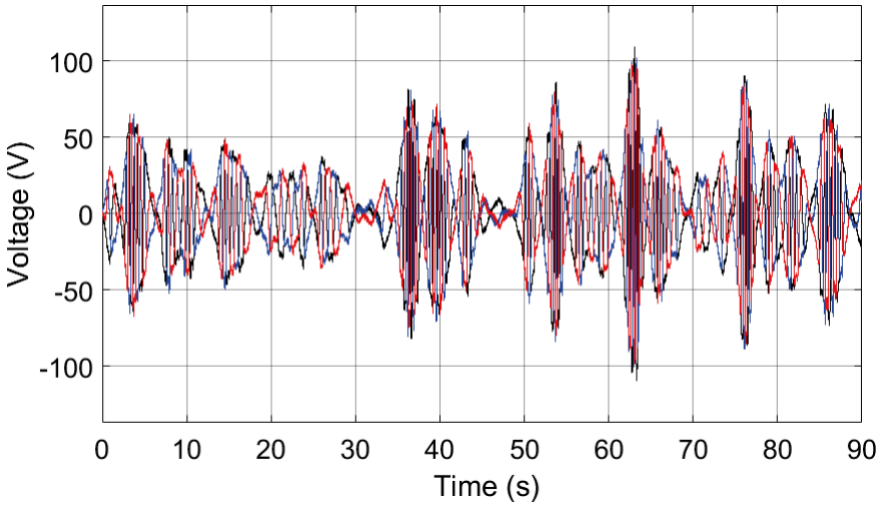

Figure 4. Three-phase voltage output of the linear permanent-magnet generator (LPMG) measured across 4.9 Ω resistive load.

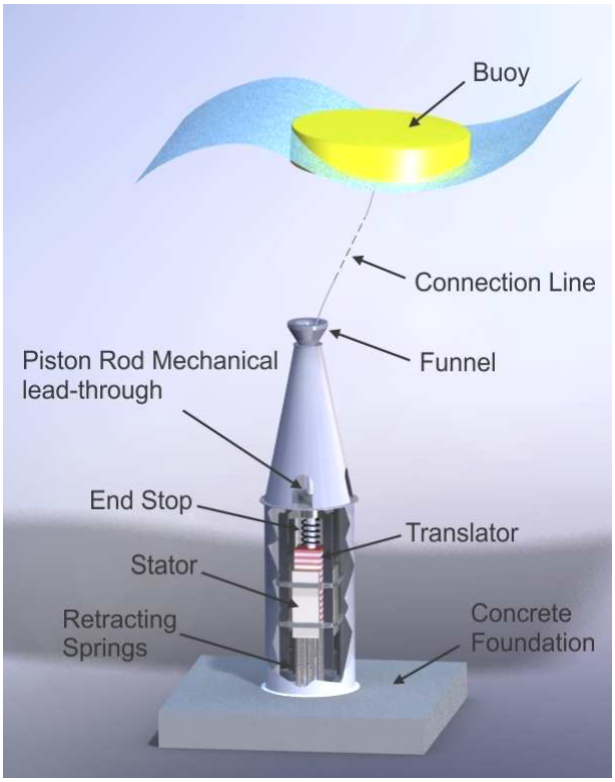

Figure 5. Schematic of Uppsala University (UU)'s WEC. Reproduced with permission from [30].

A single WEC is modelled in the Matlab/Simulink environment [31] as a two-body system combining the hydro-mechanical model of the buoy motion based on the Cummin's equation and the generator dynamics including electrodynamic forces due to the currents in the stator through a so-called wire force (see below). The WEC schematic is shown in Figure 5 and the forces acting on both buoy and translator are depicted in Figure 6. Thus, the dynamics of the WEC is given by the following two equations:

$$m_b \ddot{z}_b = F_e - F_r - F_h - F_{gb} + F_b - F_w \tag{6}$$

$$m_t \ddot{z}_t = F_w - F_d - F_{gt} + F_{es} \tag{7}$$

where m_b and m_t are the buoy and translator mass respectively, z_b and z_t denote the buoy and translator displacements, F_e is the excitation force, F_r is the radiation force, F_h is the hydrostatic stiffness force, F_{gb} and F_{gt} are the gravity forces of the buoy and the translator respectively, F_b is the buoyancy force, F_w is the wire force used for coupling between the buoy and the translator motion, F_d is the electromagnetic damping force and F_{es} is the end stop spring force. For a detailed definition of all forces, the reader is referred to [31,32]. The WEC modeling parameters are given in Table 4 The model has been validated in a number of offshore experiments, see e.g., [33,34].

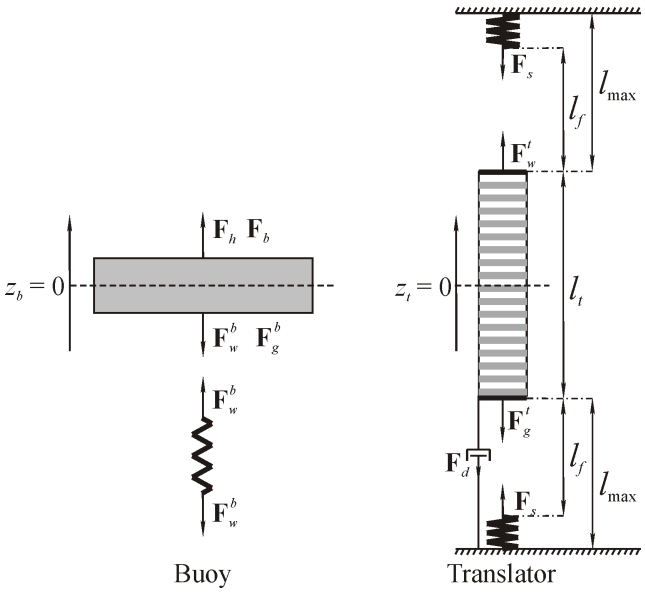

Figure 6. Forces acting on the buoy and translator. Reproduced with permission from [32].

Table 4. WEC modeling parameters. Reproduced with permission from [32].

Parameter	Value
Mass of translator (kg)	9000
Length of translator (m)	3
Length of stator (m)	2.16
End stop spring coefficients (kN/m)	270
Wire rope spring coefficient (kN/m)	833
Free stroke length (m)	0.75
Maximum stroke length (m)	1.2
Mass of buoy (kg)	4400
Buoy radius (m)	3
Moonpool radius (m)	2.3
Installed capacity at 5 kW/m (kW) [35]	30

Waves are obtained using the modified JONSWAP spectrum given in Equation (5), where the significant wave height H_S is the average significant wave height taken for two locations L1 and L4 (Figure 2.) and for two seasons—summer and winter (Table 3). Summer and winter are considered due to the extrema (minimum and maximum) of the average significant wave height. Moreover, from the grid perspective, in summer more solar PV power is available, whereas in winter more wave power could be used. Let us note that the deployment depth for UU's WEC is up to 50 m, therefore a WPF cannot be deployed at the exact location L4, but closer to shore.

The wave time series for a given significant wave height are calculated using the linear superposition of individual waves of different amplitudes A_n and angular frequencies ω_n with a random phase shift φ_n, i.e.,

$$\eta(t) = \sum_{n=1}^{\infty} A_n \cos(\omega_n t + \varphi_n) \tag{8}$$

where $\eta(t)$ is the water surface elevation at the given location (location of WEC) and the random shift φ_n is uniformly distributed on $[0, 2\pi]$. The wave amplitudes are derived from the wave power spectrum $S(\omega)$ by the formula

$$A_n = \sqrt{2S(\omega_n)\, d\omega} \tag{9}$$

where $d\omega$ is the angular frequency increment. Then the corresponding excitation force is found as

$$F_e = f_e(t) * \eta(t) \approx \sum_{n=1}^{\infty} \left|\hat{f}_e(\omega_n)\right| \cdot A_n \cos(\omega_n t + \varphi_n + \psi_n + \varepsilon_n) \tag{10}$$

where $f_e(t)$ is the impulse response function of the excitation force, and $\hat{f}_e(\omega) = \left|\hat{f}_e(\omega)\right| \cdot e^{j(\omega t + \psi)}$ is its transfer function; ε_n is the eventual phase shift due to the distance between WECs in the WPF. This approach is illustrated in Figure 7.

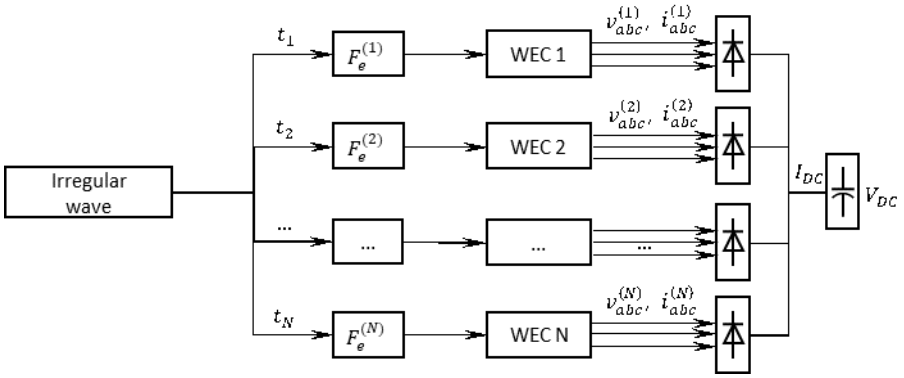

Figure 7. Schematic of wave to DC-link wave power farm model. Reproduced with permission from [31].

Since the focus of the current paper is on the impact of wave power on the power system (distribution grid) of the islands, no hydrodynamic interaction between WECs is employed here. Instead, we assume that the same incident wave reaches the WECs at different time instants with a constant time shift of 10 s. This is assumed to reduce the intermittency of the output power.

The WPF is modeled as several (two to ten) WECs connected in parallel. Three phase currents are rectified and connected to a common DC bus. The DC link voltage depends on the sea state and can be kept constant through the year or adjusted based on an optimal value [36]. In the presented simulations the DC link voltage is 80 V and is kept constant regardless of the number of WECs connected to the DC link and the season. This approach was chosen since there is no big difference between sea states in the locations L1 and L4 and between seasons.

The electrical infrastructure chosen for a WPF consisting of several of UU's WECs is presented in Figure 8. This layout was considered the most suitable since it reduced cabling and led to a more efficient power transmission to shore for WECs with a moderate installed power capacity [36].

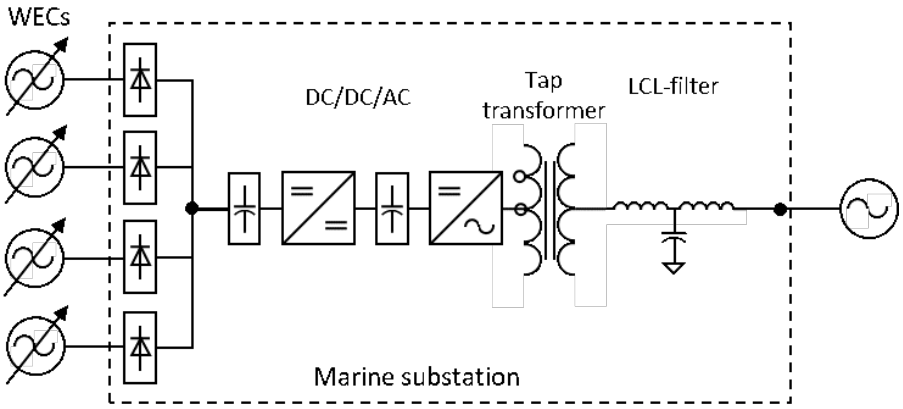

Figure 8. One-line diagram of electrical layout of a wave power farm (WPF) consisting of several of UU's WECs.

2.3. Grid Integration Models of WPF

The large scale integration of DG into the power grid emerged mostly from stimulating policies in the 21st century regarding renewable energy sources. Due to the variable nature of wave energy and the resulting electricity generated, there are many technical aspects of WEC DG integration to consider [37], such as influence on voltage rises, changes in power flows and losses, short-circuit currents and protection schemes and power quality in terms of the European Norm EN 50160, including voltage variations, flicker injection, harmonic distortion, mostly on the grid connection point and its close surroundings, as well as the general influence of the increasing level of WEC DG integration on the reliability and stability of the overall power system supply.

Integration of the DG with the passive distribution network results in a change in power flows as well as a change in power losses, depending on the current output power of the DG and the current load on the feeder. The reduction of power (energy) losses after the integration of the DG can be defined as [37]:

$$\Delta E_{loss} = \sum_{s=1}^{N} \int_{0}^{T} G_s(t) \cdot [2 \cdot L_s(t) - G_s(t)]\, dt \tag{11}$$

where ΔE_{loss} is the change in energy losses, N_s is the number of feeder sections,L_s is the downstream load (consumption) and G_s is the downstream generation of the DG on the feeder section s.

As long as the expression in parenthesis stays positive, for all timesteps t and sections of the feeder s, power losses are reduced. However, depending on this ratio, DG can cause an increase in power losses.

The most common limiting factor that occurs in the case of large-scale integration of the DG into the distribution network is voltage rise [1]. This voltage rise depends on the active power injection and position of the DG along the feeder; therefore, the voltage rise magnitude in the case of a uniformly distributed load on the feeder can be expressed as [37]:

$$\Delta u_{gen} = \begin{cases} L \cdot \frac{R \cdot P_{gen}}{U_{nom}^2}, & L \leq L_{gen} \\ L_{gen} \cdot \frac{R \cdot P_{gen}}{U_{nom}^2}, & L > L_{gen} \end{cases} \tag{12}$$

where L is location on the feeder, R is the source resistance at the terminals of the generator, P_{gen} is the generator active power and U_{gen} is the nominal voltage.

Since DGs (and WECs in particular) are a relatively new concept in electricity generation, they introduce problems to distribution network operation that have been so far non-existent. To assess the possibility of DG integration into the distribution network, the term "hosting capacity" is used. The hosting capacity of the distribution network can be defined as the amount of energy from the DG that the distribution network can absorb

at the point of common coupling (PCC) without violation of the system's operational constraints. Various hosting capacity enhancement methods are available but the most frequent limiting factor for the further integration of DG into the distribution network is the voltage rise, therefore there is significant ongoing related research. Typically, grid operators limit voltage level variability in the range of ±10% from its nominal value and most efforts are focused on voltage control.

There is a wide range of research available on this subject, incorporating different methods. The authors in [38] studied how different voltage regulation methods and network topology manipulations, such as off-load tap changers (OLTCs) on transformers, parallel connected inductors, generator power factor change, network reinforcement and network upgrades, influence the hosting capacity of the distribution network. Further, in [39], the authors analyzed the influence of small single-phase DG units on overvoltage and voltage imbalance when integrated into the low voltage distribution network. The influence of network reconfiguration and the utilization of energy storage systems on the hosting capacity of a medium voltage distribution network can be found in [40]. Network reinforcement can also increase hosting capacity by placing new parallel elements next to existing ones or increasing the network element loadability. In [41], operating range, technical potentials and economic efficiency compared with conventional network reinforcement were calculated for the cost efficient grid integration of the DG in the distribution network. In [42], the authors investigated how the reactive power management, different residential load characteristics and two different network setups influenced the distribution network hosting capacity for DG. Capitanescu et al. [43] investigated how an active network management scheme can increase the distribution network hosting capacity by means of network reconfiguration using remote-controlled switches. A combined method for hosting capacity evaluation with OLTCs and static var compensation under the uncertain generation of DG and load consumption is presented in [44].

3. Case Study of Possible WEC Integration on an Adriatic Island: Results

This section describes the power flow analysis model of the daily operation of a low voltage distribution network with an integrated WPF applied to conditions typical for a small Adriatic (Mediterranean) island with low wave energy potential and variable consumption throughout the year, namely, low electricity demand (consumption) during the winter period (off tourist season) and high electricity demand (consumption) during the summer period (tourist season).

WPF generation (1-s time resolution) estimated by the model for the two locations (L1 and L4 in Figure 2) and two seasons (summer and winter in Table 3) was used to analyze the possibility of deployment of a WPF with and without PV systems and BESS technologies into the low voltage distribution network. The daily electricity generation for various numbers of WECs in a WPF, generated by the model of WPF, for locations L1 and L4 and for both summer and winter season are given in Figure 9.

The power network (grid) model into which the WPF/PV/BESS were integrated is the Institute of Electrical and Electronics Engineers (EEE) European Low Voltage Test Feeder (LVTF), a 11/0.416 kV AC low voltage unbalanced distribution network. The IEEE European LVTF was developed to represent a 50 Hz test feeder at the low voltage level of 416 V (phase-to-phase), typical in European low voltage distribution systems. The test system consisted of an 11/0.416 kV transformer, 907 buses, 905 lines and 55 loads presented with 55 consumption profiles of household-size consumers with a one-minute time resolution over 24 h. This enabled time-series load flow analysis over a one-day period or static load flow analysis at specific moments in a day. The low voltage 416 V network was connected to an 11 kV upstream network via a three-phase transformer rated at 0.8 MVA and a delta/grounded-wye connection (Dyn) of windings. The resistance and reactance of the transformer impedance were 0.4% and 4%, respectively. The reader can find more details on the IEEE LVTF in [45].

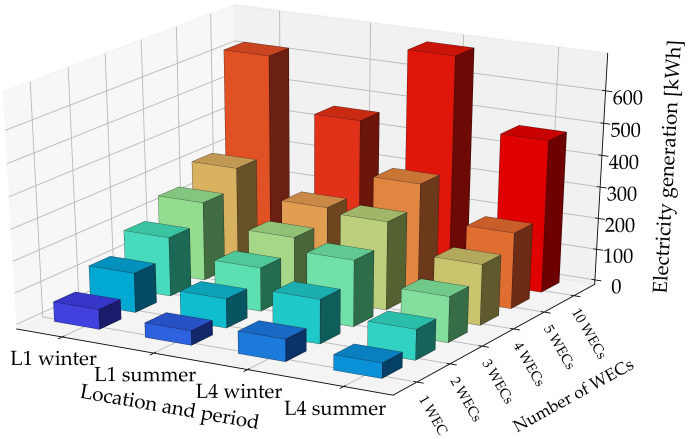

Figure 9. Daily electricity generation for various number of WECs in a WPF on locations L1 and L4, and summer and winter seasons.

The original consumption profile of the feeder was adjusted to represent the winter period (off tourist season) and summer period (tourist season). Winter-period consumption consisted of 14 households (nearly every fourth is active), describing the consumption of the domestic population on the island, which is multiple times smaller than the consumption during the summer period—influenced by the tourist season. The summer-period consumption profile considered 55 households (original number and consumption profile of the feeder) to encompass the increase in load during the summer period, mainly influenced by the power consumption by air conditioning systems. The power factor of each household was set to 0.95 lagging (inductive). The winter-period and summer-period consumption profiles of the feeder are shown in Figure 10. Furthermore, the 11-kV upstream network in which the LVTF is connected to a swing bus was represented with a three-phase short-circuit power of 35 MVA, a single-phase short circuit power of 95.26 kVA (isolated 11 kV side) and a reference voltage of 1.05 p.u. These settings were provided by the distribution system operator for the island of Vis, Croatia, and represent realistic island power network input data, located near the location L4.

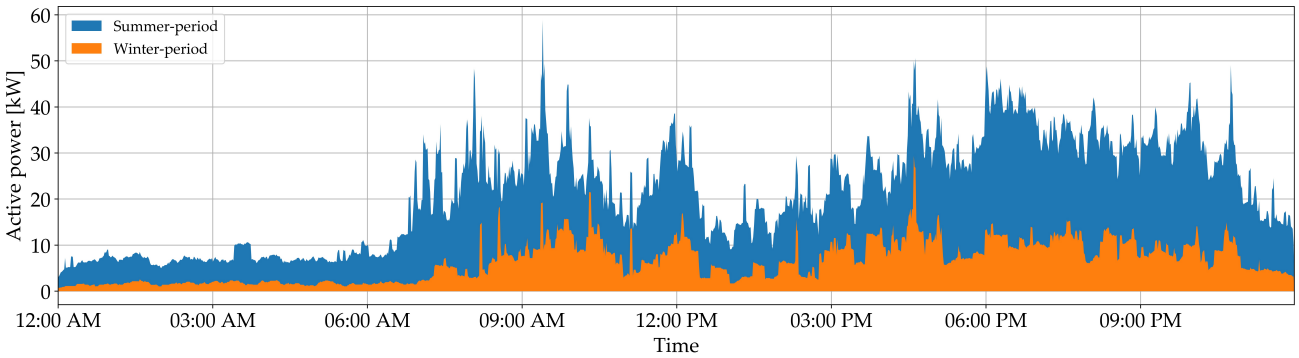

Figure 10. Winter-period and summer-period consumption profiles of the test feeder.

WECs (a WPF) were connected to the electrically most-distant bus in the LVTF (bus 881), also visible in Figure 11. Each WEC was connected as a three-phase generator model with a unity power factor.

Operation of the LVTF was carried out for the following case studies:

Case study 1—winter-period (off tourist season) consumption profile of distribution feeder with various numbers of WECs in a WPF installed on location L4 with winter-period generation profile and with or without BESS.

Case study 2—optimal number of WECs (size of WPF) needed to achieve nearly zero electricity exchange with upstream network, as determined in case study 1, were installed

on location L4 with the summer-period WPF generation profile, summer-period (tourist season) consumption profile of distribution feeder, integrated 12 PV systems (accounting for about 20% share of households) with the summer-period generation profile and with or without BESS.

Case study 3—optimal number of WECs (size of WPF), as determined in the case study 1, are installed on location L4 with winter-period WPF generation profile, winter-period consumption profile of distribution feeder, integrated 12 PV systems (accounting for about 20% share of households) from case study 2 (winter period generation profile) and with/without BESS.

Case study 1 was carried out to determine the optimal number of WECs needed to achieve nearly zero electricity exchange of the LVTF and the upstream network. Case study 2 was performed to point out the advantages and possible problems in operation that can occur when integrating PV systems with this feeder and to alleviate the increase in consumption during the summer period (tourist season). The same situation was studied with winter-period consumption and generation profiles in case study 3 in order to determine the influence of overall electricity generation from both WPF and PV systems during the winter period (off tourist season) as well.

Time-series (load flow calculations) simulations of LVTF operation were carried out in OpenDSS, an open-source power system analysis software, driven through the Component Object Model (COM) interface with the Python programming language [46]. Each simulation is carried out for one-day operation with 1-min time resolution, resulting in 1440 load flow calculations.

A one-line diagram of the LVTF used for case studies carried out in this paper with indicated 11/0.416 kV substation, spatial distribution of 55 household-size consumers (1 to 55), 12 PV systems (PV1 to PV12) and the WPF and BESS is presented in Figure 11.

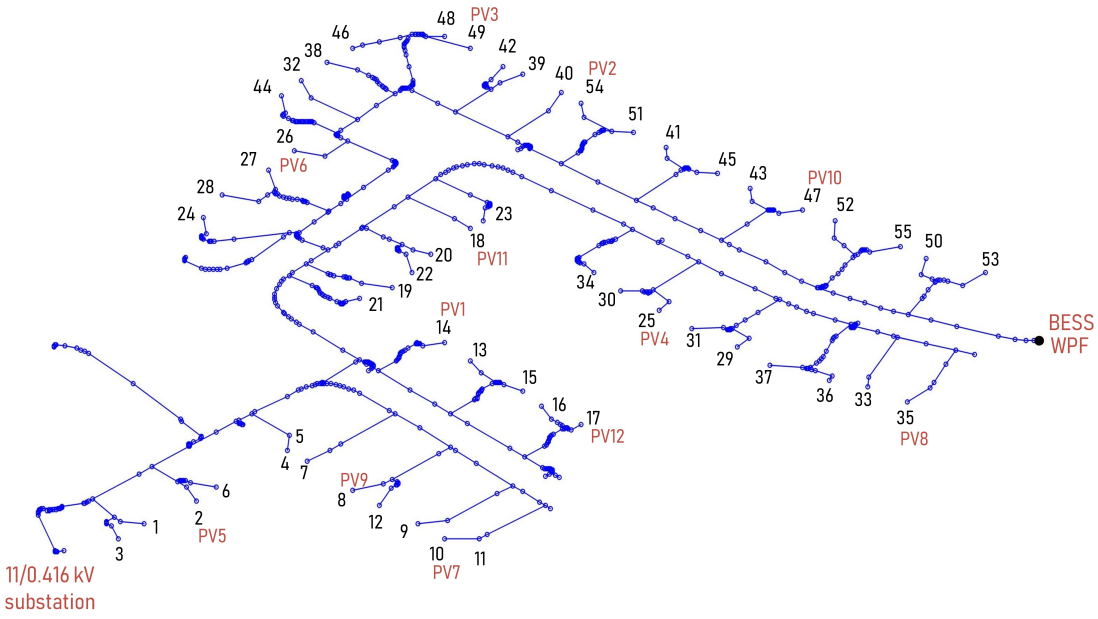

Figure 11. One-line diagram of the LVTF.

3.1. Case Study 1–Optimal Number of WECs in WPF for Winter Electricity Demand (Consumption)

The task of case study 1 was to determine the optimal number of WECs in a WPF to achieve nearly zero electricity exchange with the upstream distribution network for winter-period (off tourist season) consumption.

Table 5 shows the observed parameters extracted after the simulations of daily operation. It is visible from the results that two WECs in a WPF results (bolded column in table) in the lowest (closest to zero) net daily import of 15.66 kWh of electricity from the upstream distribution network, which was therefore considered the optimal number of WECs in a WPF integrated into the LVTF. Furthermore, it is visible that minimum voltage, active and reactive energy (bolded) losses occurred in the case of 1 WEC in a WPF (bolded), rather than for the two WECs, which is considered the optimal number of WECs, even though the lost active and reactive energy was close to the minimum. The highest voltage occurred on the bus 881, PCC bus of WPF and LVTF, and the highest active and reactive power losses were observed in the case of 10 WECs (bolded) in a WPF due to its having the largest active power injection, as expected.

Table 5. Results of the daily operation simulation for case study 1–optimal number of WECs in a WPF for the winter season (consumption). LVTF: Low Voltage Test Feeder.

Number of WECs in WPF	0 (ref)	1	2	3	4	5	10
WPF active energy generation (kWh)	0	72.06	**140.35**	207.15	279.34	350.04	702.89
Net LVTF active energy exchange (kWh)	−155.47	−83.55	**−15.66**	50.56	121.86	191.45	535.29
Net LVTF reactive energy exchange (kVArh)	−51.01	−51.05	**−51.14**	−51.30	−51.52	−51.81	−54.17
Upstream active energy flow from LVTF (kWh)	0	11.20	**40.62**	79.88	134.40	196.52	535.38
Downstream active energy flow into LVTF (kWh)	155.47	94.75	**56.28**	29.32	12.54	5.07	0.10
LVTF total active energy losses (kWh)	1.02	**0.92**	**1.08**	1.44	2.07	2.94	**10.74**
LVTF total reactive energy losses (kVArh)	0.25	**0.20**	**0.22**	0.30	0.44	0.65	**2.62**
Minimum voltage during simulations (p.u.)	**1.002**	1.003	**1.003**	1.005	1.007	1.009	1.017
Minimum voltage on bus	899	899	**899**	899	899	899	899
Minimum voltage in timestep	619	620	**620**	620	620	620	621
Maximum voltage during simulations (p.u.)	1.064	1.066	**1.069**	1.07	1.072	1.074	**1.081**
Maximum voltage on bus	868	881	**881**	881	881	881	881
Maximum voltage in timestep	619	621	**619**	619	619	619	619

Since the output power data of the WECs (WPF) is generated in 1-s time resolution, for better visibility, only the one-hour output power profile of a WPF consisting of two WECs (the optimal number) at the PCC with the LVTF is shown in Figure 12.

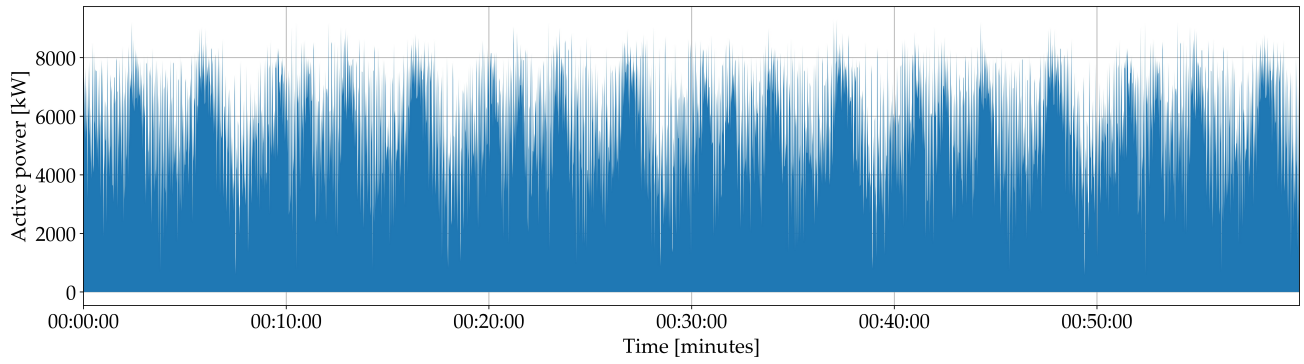

Figure 12. One-hour output power of WPF consisting of 2 WECs at the point of common coupling (PCC) with LVTF.

There is large intermittency in the output power profile, which is result of the nature of the WEC operation. To mitigate this behaviour, a smoothing technique was applied in this paper's case studies, using a BESS installed at the PCC of the WPF and the LVTF, to smooth the output power profile.

Table 6 presents the technical characteristics of the BESS connected at the PCC of the WPF and LVTF. The BESS's technical characteristics were determined through a trial-and-error method to effectively achieve the effect of smoothing the active power output at the PCC of the WPF and the LVTF.

Table 6. Technical characteristics of battery energy storage system (BESS) integrated at the WPF PCC.

Parameter	Value
Battery capacity (kWh)	10
Nominal apparent/active power (kVA/kW)	5
Power factor	1
Initial battery state of charge (SOC) [%]	70
Minimum battery SOC (%)	20
Idling (no-load) losses of active power (%)	0.1
Battery charging efficiency (%)	95
Battery discharging efficiency (%)	95

The dispatch profile of the BESS was generated manually so that the output power of the WPF at the PCC varied ±10% from the daily mean output power. For example, for a daily mean WPF output power of 5.867 kW, the net output power at the PCC would vary from 5.281 kW to 6.454 kW. Figure 13 gives the one-hour dispatch (1 s time resolution) profile of the BESS for the optimal case (two WECs in a WPF), to achieve the variability of ±10% from the daily mean output power, where negative values represent charging power whereas positive values represent discharging power.

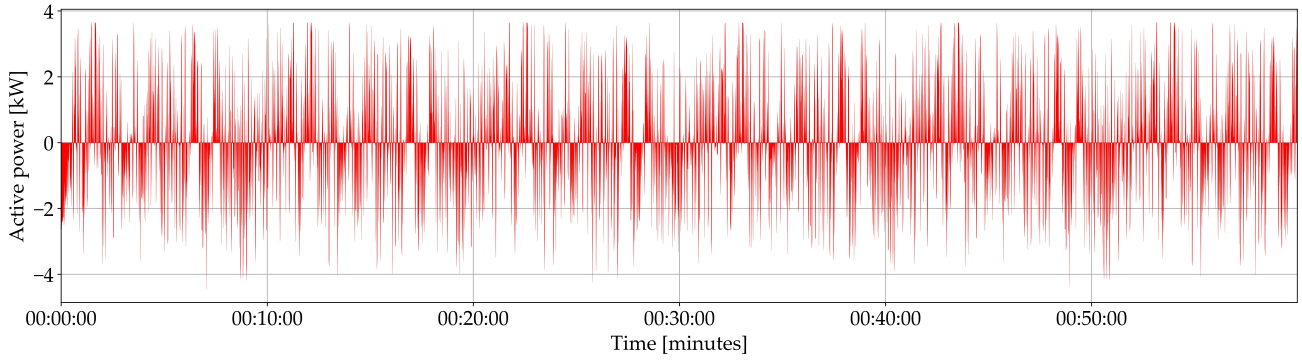

Figure 13. One-hour dispatch profile of BESS.

The results of the time-series simulations are presented in Figure 14, which shows the active power exchange of the LVTF with the upstream network at the swing bus for the following scenarios in case study 1: reference case (load only, no WPF, no BESS); WPF with two WECs only (2 WECs only); and the combination of WPF with two WECs and BESS (2 WECs + BESS).

The results presented in Figure 14 show that in scenarios where a WPF consisting of two WECs was operating, the exchanged active power was shifted upwards, resulting in alternating upstream and downstream active power flows during the time of the day, depending on the current consumption of loads. In a scenario using BESS installed at the WPF PCC (2 WECs + BESS scenario), the smoothing technique proved to be effective when alleviating the intermittency, and the generation profile trend was preserved.

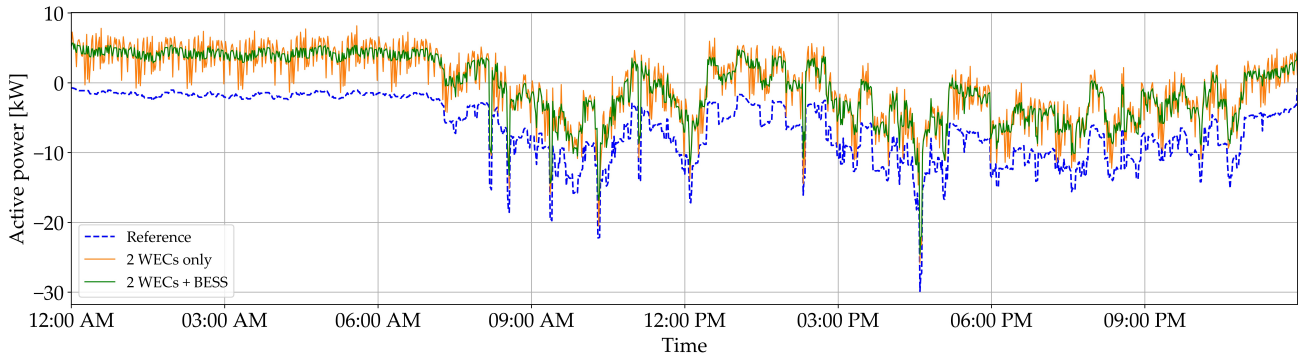

Figure 14. Active power exchange of the LVTF and upstream network at the swing bus for various scenarios in case study 1.

Figure 15 gives the voltage profiles of each phase (L1, L2 and L3) at the WPF (and BESS) PCC bus (bus 881) for the following scenarios in case study 1: reference case (load only, no WPF, no BESS); WPF with WECs only (2 WECs only); the combination of WPF with two WECs and BESS (2 WECs + BESS).

Figure 15. Voltage profiles at the WPF PCC bus for various scenarios in case study 1.

The results show that there was a continuous voltage rise (in comparison to the levels for the reference case) on the WPF PCC during the day caused by the injection of active power. The smoothing technique using the BESS, as in the case for the active power exchange, also preserved the voltage profile trend while alleviating the intermittency caused by the nature of the active power profile.

3.2. Case Study 2–Operation of WECs (WPF) and PV Systems during Summer Season (Consumption)

In case study 2 we analyzed the operation of the LVTF during the summer period, presented with increased consumption (in comparison to winter-period consumption used in case study 1) due to the tourist season, as well as the additional electricity generation

by the household-sized PV systems integrated at various locations in the LVTF. This case study points out the advantages and possible problems in operation that can occur when integrating PV systems, which is a very likely situation to occur due to large solar energy potential of this region, in this feeder and the increase in consumption during the tourist (summer-period) season.

This case study considers that the optimal number of WECs in a WPF (two), as determined in case study 1, are installed on location L4 and presented with a summer-period generation profile. Furthermore, the consumption profile of the distribution feeder is presented with increased consumption during the tourist season, as given in Figure 10, and integrated PV systems are presented with the summer-period generation profile. Finally, operation with and without BESS was studied. To analyze the worst-case scenario, a scenario with 10 WECs in WPF and with generation of PV systems was also carried out.

There were a total of 12 single-phase (household size) PV systems integrated into the feeder (accounting for about a 20% share of households) with an installed power of 3.6 kVA. PV systems were distributed evenly across all three phases (four PV systems on each phase) and placed randomly in the LVTF. Technical characteristics and locations of PV systems are given in Table 7, whereas Figure 16 shows solar irradiance and PV module temperature profiles used for the summer period (used in case study 2) and the winter period (used in case study 3). Solar irradiance and PV module temperatures representing field measurements were acquired from [47] for the island of Vis, Croatia.

Table 7. Technical characteristics and locations of PV systems in the distribution network.

Parameter	Value
Locations (bus) in phase L1	289, 502, 861, 900
Locations (bus) in phase L2	47, 248, 522, 639
Locations (bus) in phase L3	208, 327, 337, 835
Inverter rated apparent power (kVA)	3.6
Power factor	1
PV array installed power (kWp)	4
Power temperature coefficient (%/°C)	0.4
Inverter efficiency (%)	98
Cut-in/cut-out power (%)	1

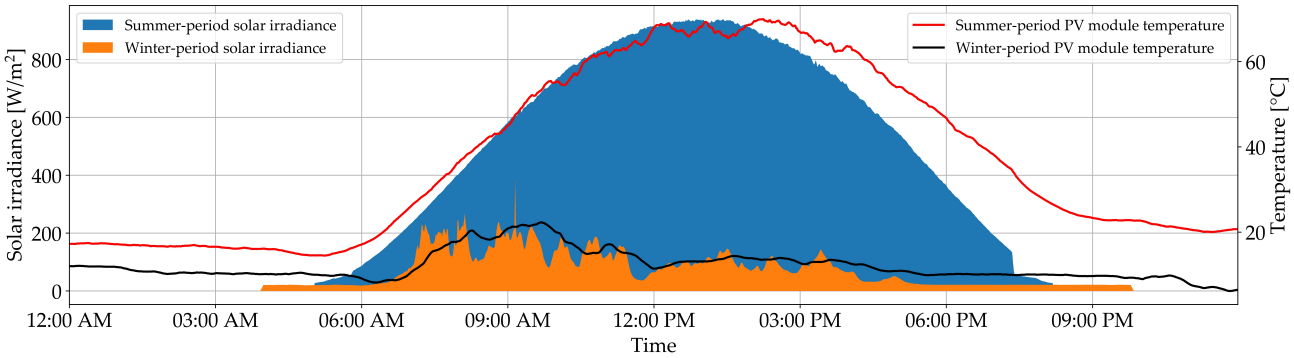

Figure 16. Solar irradiance and photovoltaic (PV) module temperature profile used for summer and winter periods.

Results of the time-series simulations are presented in Figure 17, which shows the active power exchange of the LVTF with the upstream network at the swing bus for the following scenarios in case study 2: reference case (load only, no WPF, no PV, no BESS); WPF with two WECs in combination with PV systems (2 WECs + PV); the combination of a WPF with two WECs; PV systems and BESS (2 WECs + BESS + PV); worst case scenario of a WPF with 10 WECs in combination with PV systems (10 WECs + PV).

For the scenario of a WPF with two WECs and PV systems, there was a significant upstream active power flow during the daytime, caused by PV system generation, whereas

the entire active power profile was shifted upwards by the WPF generation, and even the consumption of the feeder was increased due to the tourist season. Like in the previous case, the integrated BESS created a smoothed active power profile. In the worst-case scenario of a WPF with ten WECs in combination with PV systems, there was an upstream active power flow for most of the time during the day.

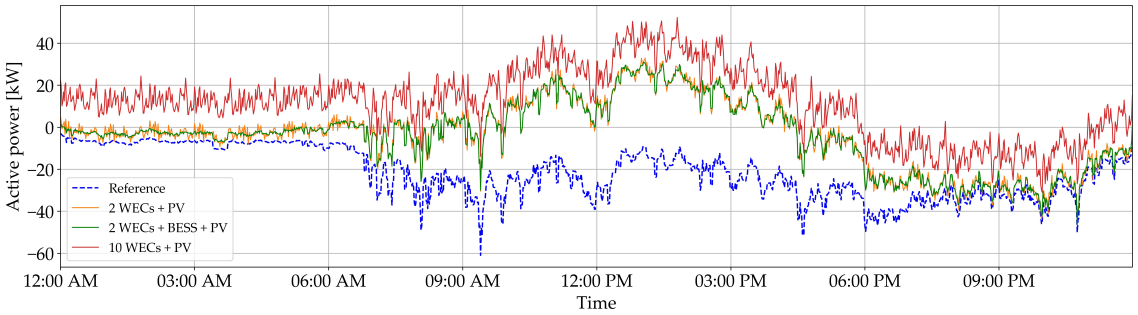

Figure 17. Active power exchange of the LVTF and upstream network at the swing bus for various scenarios in case study 2.

Figure 18 presents voltage profiles of each phase (L1, L2 and L3) at the WPF (and BESS) PCC bus (bus 881) for the following scenarios in case study 2: reference case (load only, no WPF, no PV, no BESS); WPF with two WECs in combination with PV systems (2 WECs + PV); the combination of WPF with two WECs; PV systems and BESS (2 WECs + BESS + PV); worst case scenario of WPF with 10 WECs in combination with PV systems (10 WECs + PV). Like in a case study 1, there was a voltage profile rise that was present continuously during the day, caused by the generation, even though there was no distinguishable rise in voltage during the daytime caused by PV system generation. Furthermore, in the worst-case scenario, voltage levels approached the upper voltage margin of 1.1 p.u., which can be exceeded in case of further integration of RES-based generation.

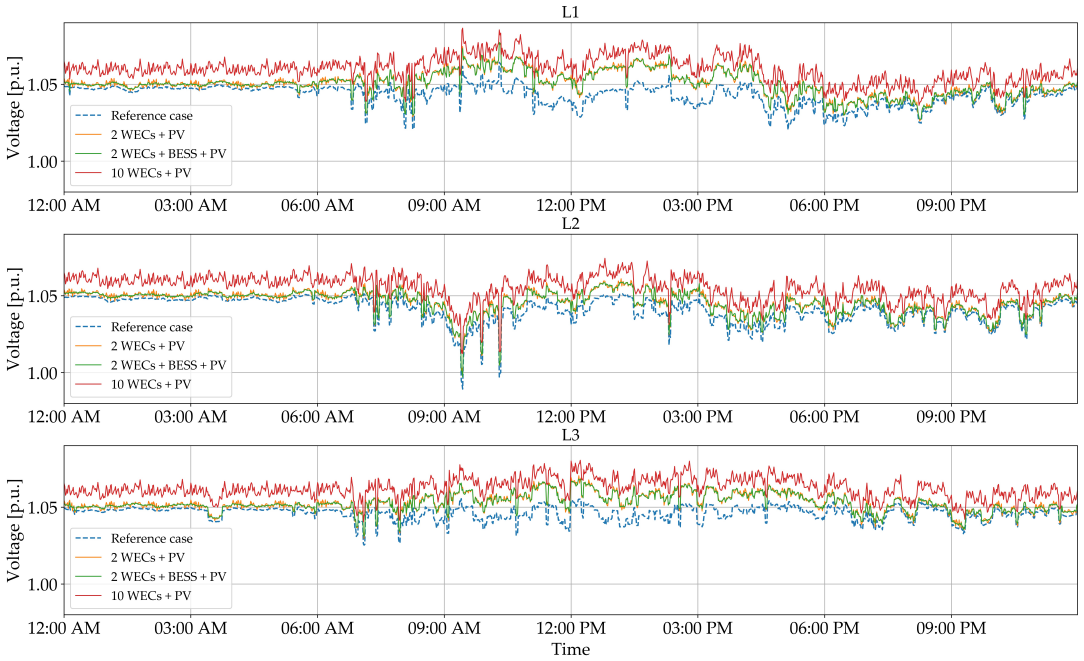

Figure 18. Voltage profiles at the WPF PCC bus for various scenarios in case study 2.

Results given in Table 8 present the parameters extracted after the daily operation simulation for case study 2 scenarios: reference case (load only, no WPF, no PV, no BESS); WPF with two WECs in combination with PV systems (2 WECs + PV); the combination of WPF with two WECs, PV systems and BESS (2 WECs + BESS + PV); worst case scenario of

WPF with 10 WECs in combination with PV systems (10 WECs + PV). Results with two WECs in combination with PV systems with or without BESS, considered as optimal cases based on achieving net zero electricity exchange with the grid, have been bolded in the table. The highest voltage occurred on bus 881, the PCC bus of WPF and LVTF for the case of 10 WECs (bolded) in a WPF due to the largest active power injection, as expected.

Table 8. Results of the daily operation simulation for case study 2.

Number of WECs in WPF	0 (Reference)	2 WECs + PV	2 WECs + BESS + PV	10 WECs + PV
WPF active energy generation (kWh)	0	**101.02**	**101.02**	476.83
Net LVTF active energy exchange (kWh)	−522.56	**−86.16**	**−89.98**	281.64
Net LVTF reactive energy exchange (kVArh)	−171.68	**−172.60**	**−172.57**	−174.86
Upstream active energy flow from LVTF (kWh)	0	**108.96**	**106.01**	345.53
Downstream active energy flow into LVTF (kWh)	522.56	**195.12**	**195.99**	63.89
LVTF total active energy losses (kWh)	5.07	**3.77**	**3.72**	7.55
LVTF total reactive energy losses (kVArh)	1.59	**0.96**	**0.95**	1.83
Minimum voltage during simulations (p.u.)	0.982	**0.994**	**0.993**	0.999
Minimum voltage on bus	639	**639**	**639**	639
Minimum voltage in timestep	567	**567**	**567**	567
Maximum voltage during simulations (p.u.)	1.064	**1.077**	**1.077**	**1.087**
Maximum voltage on bus	873	**881**	**881**	881
Maximum voltage in timestep	619	**619**	**619**	567

The results show that integration of BESS has minimal influence on the observed parameters while the effect of intermittency is mitigated, as visible in Table 8.

3.3. Case Study 3–Operation of WECs (WPF) and PV System during Winter Season (Consumption)

In case study 3, we studied the operation of the LVTF with the same generation units as in case study 2 but with the seasonal conditions of case study 1 (the winter period). Therefore, the following situation was presented—two integrated WECs (the optimal number from case study 1) in a WPF installed on location L4 with the winter-period generation profile (Figure 12), winter-period consumption profile (Figure 10) of LVTF, 12 integrated PV systems (accounting for about a 20% share of households) from case study 2, with the winter-period consumption profile (input profiles presented in Figure 16) and with/without BESS. In comparison to case study 1, the task of this case study was to analyze the influence of additional generation from PV systems during the winter period.

The results shown in Figure 19 indicate the active power exchange of the LVTF with the upstream network at the swing bus for the following scenarios in case study 3—reference case (load only, no WPF, no PV, no BESS); WPF with two WECs in combination with PV systems (2 WECs + PV); the combination of WPF with two WECs, PV systems and BESS (2 WECs + BESS + PV); worst case scenario of WPF with 10 WECs in combination with PV systems (10 WECs + PV).

For the scenario of a WPF with two WECs and PV systems, there was an upstream active power flow throughout the day and the generation from the PV systems did not significantly influence the upstream power flow. Furthermore, the entire active power profile was shifted upwards by the WPF generation in comparison to the reference case. As in the previous case study, the integrated BESS smoothened the active power profile. In the worst-case scenario of a WPF with 10 WECs in combination with PV systems, there was a significant upstream active power flow during the entire day.

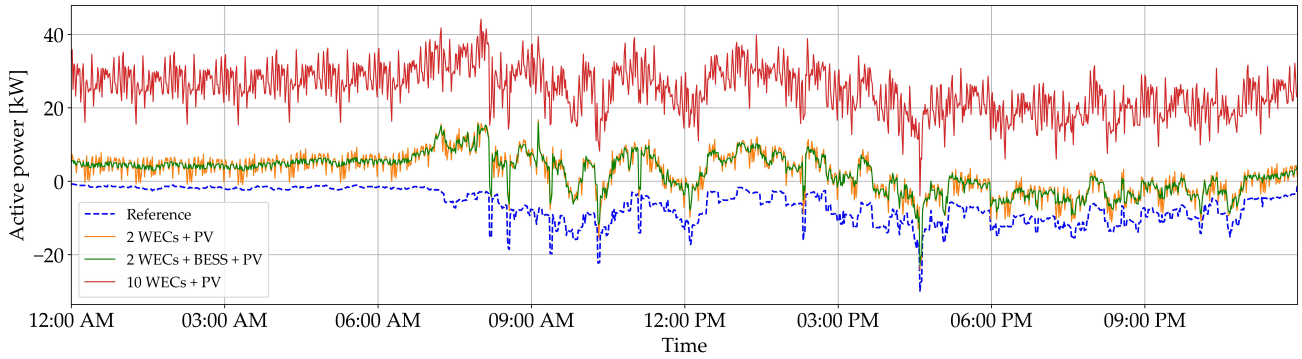

Figure 19. Active power exchange of the LVTF and upstream network at the swing bus for various scenarios in case study 3.

Figure 20 presents the voltage profiles of each phase (L1, L2 and L3) at the WPF (and BESS) PCC bus (bus 881) for the following scenarios in case study 3—reference case (load only, no WPF, no PV, no BESS); WPF with two WECs in combination with PV systems (2 WECs + PV); the combination of a WPF with two WECs; PV systems and BESS (2 WECs + BESS + PV); worst case scenario of WPF with 10 WECs in combination with PV systems (10 WECs + PV).

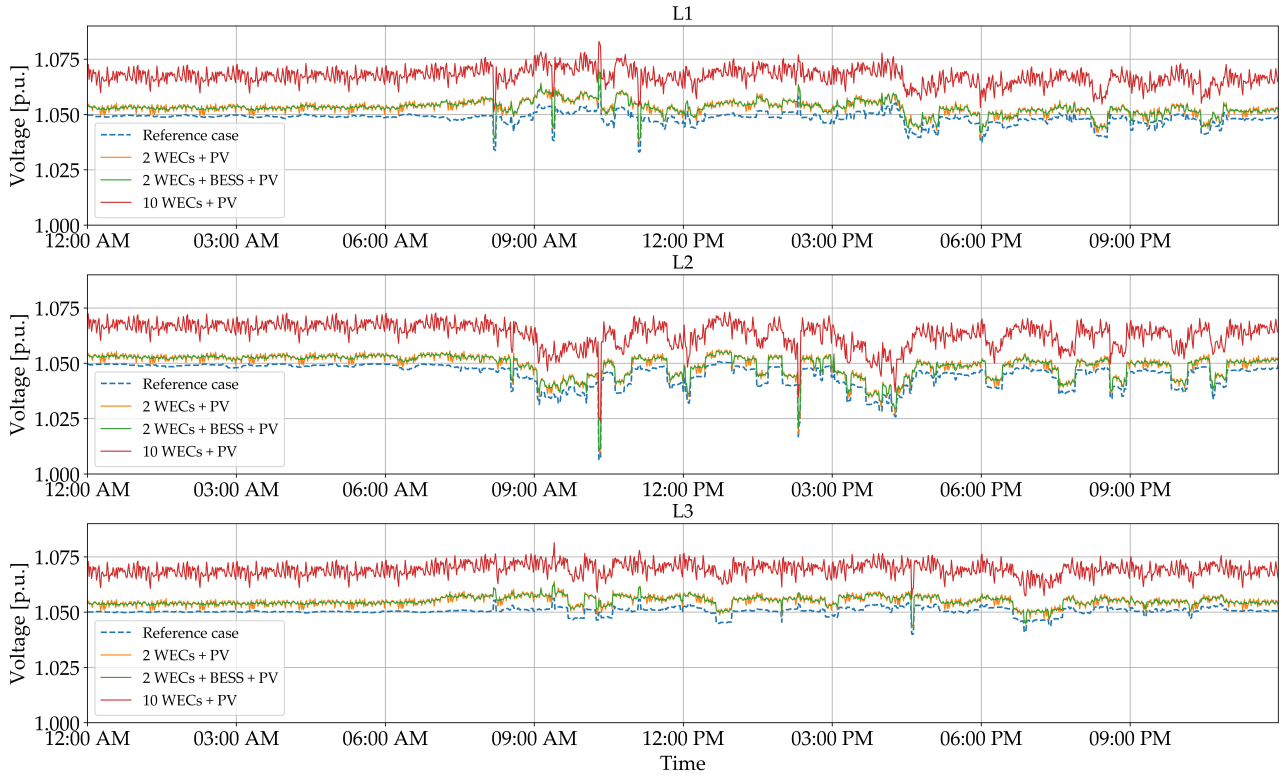

Figure 20. Voltage profiles at the WPF PCC bus for various scenarios in case study 3.

As in case studies 1 and 2, there was a voltage profile rise that was present continuously during the day caused by the active power generation, even though there was no distinguishable voltage rise during the daytime when PV systems were generating power.

The results given in Table 9 present the parameters extracted after the daily operation simulation for case study 2 scenarios—reference case (load only, no WPF, no PV, no BESS); WPF with two WECs in combination with PV systems (2 WECs + PV); combination of a WPF with two WECs; PV systems and BESS (2 WECs + BESS + PV); worst case scenario of a WPF with 10 WECs in combination with PV systems (10 WECs + PV). The results of scenarios with two WECs in combination with PV systems with or without BESS—

considered to be optimal cases based on achieving net zero electricity exchange with the grid—have been bolded in the table. The highest voltage occurred on bus 881, PCC bus of WPF and LVTF for the case of 10 WECs (bolded) in a WPF due to the largest active power injection, as expected.

Table 9. Results of the daily operation simulation for case study 3.

Number of WECs in WPF	0 (Reference)	2 WECs + PV	2 WECs + BESS + PV	10 WECs + PV
WPF active energy generation (kWh)	0	**140.35**	**140.35**	702.89
Net LVTF active energy exchange (kWh)	−155.47	**52.27**	**54.20**	602.47
Net LVTF reactive energy exchange (kVArh)	−51.01	**−51.23**	**−51.23**	−54.54
Upstream active energy flow from LVTF (kWh)	0	**83.57**	**82.93**	602.53
Downstream active energy flow into LVTF (kWh)	155.47	**31.30**	**28.73**	0.07
LVTF total active energy losses (kWh)	1.02	**1.20**	**1.16**	11.62
LVTF total reactive energy losses (kVArh)	0.25	**0.25**	**0.24**	2.93
Minimum voltage during simulations (p.u.)	1.002	**1.004**	**1.006**	1.018
Minimum voltage on bus	899	**899**	**899**	899
Minimum voltage in timestep	619	**620**	**620**	621
Maximum voltage during simulations (p.u.)	1.064	**1.07**	**1.069**	**1.083**
Maximum voltage on bus	873	**881**	**881**	881
Maximum voltage in timestep	619	**619**	**619**	567

4. Economic, Environmental and Social Aspects of WPFs

4.1. Environmental Aspects of WPFs

Utilization of wave energy to generate electricity has economic, environmental and social effects. According to International Energy Agency environmental impact assessments of ocean energy converters, it is necessary to inform regulators about the potential effects of ocean energy deployment. The state of knowledge concerning environmental effects—which drives the consenting/permitting process in the marine renewable energy industry—is available in [48].

The environmental impacts of wave energy conversion devices are site- and technology-specific. Each project will have unique effects on the environment, depending on two things—the design of the device (including the size of the array) and the specific environmental characteristics of the project site. There are very few data available specifically on the environmental impacts of wave energy conversion devices, such as those presented in Boehlert G.W., et al. [49].

Environmental impact analysis (EIA) requires developers to supply comprehensive environmental data relating to baseline conditions and device installation and operation. Since WECs represent a new energy production system in deployment, there is a gap in knowledge and information available to all participants, from regulatory authorities to developers. The potential impact on the environment can vary depending on the type of system installed, according to Greaves D. et al. [50]. Wave energy extraction system are generally classified according to their working principles (attenuator, point absorber and terminator) and location (shoreline, near-shore and offshore), and EIA should cover every aspect of the installed system, according to Chen Z. et al. [51] and Falcao [26]. The main concerns are effects on the benthic community and species-specific responses to habitat change (leading to abandoning the habitat, although the area could be re-colonized, if substrate and habitats are restored to similar state), as well as the entanglement of marine mammals, turtles, larger fish and seabirds. Research in the area of environmental impacts should be focused on localized environmental impacts, including, e.g., electromagnetic field effects of subsea cables, flow alteration, sedimentation and habitat change of nearby

generation devices (Beyene A. et al.) [52], (Boehlert et al.) [49], (Uihlein A., Magagna D.) [53]. Changes to wave parameters are considered in conjunction with hydrodynamic forces, such as current velocities and resultant bed shear stress (Roberts, J.D., et al.) [54]. Chemical effects of WECs such as spills (low probability but high impact) and continuous release (fouling paints) can cause water quality interference. Noise disturbances throughout all stages of construction, operation and decommission are also possible—it is evident that these structures produce sounds that may disturb or even cause physical damage to wildlife in the vicinity and may also disturb local communities (Beyene A. et al.) [52]; (Copping, A. et al.) [48] (Margheritini, L. et al.) [55]. There may also be interference with marine animal movements and migrations. The construction of large-scale systems could disrupt breeding or feeding areas or interrupt migration routes (Margheritini, L. et al.) [55] and could also lead to collisions with moving parts of the devices, particularly turbine blades (Copping, A. et al.) [48].

There are many ways to tackle reliability concerns, since they exist in each of the following subsystems of a WEC device—structure, power conversion, mooring and grid connection components. System reliability directly effects the performance of planned and unplanned maintenance and the availability of the device to make power [56].

Among all the technologies available to convert wave energy, the point-absorber is one of the most promising solutions today, due to its ease of both fabrication and installation. The floaters of point-absorber WECs are generally exposed to harsh marine environments with great uncertainties in environmental loads, which make their reliability assessment quite challenging [57].

Maintenance can either be performed in situ or the device can be disconnected from electrical and mooring infrastructure, towed back to a sheltered site and serviced there. Execution of maintenance is dependent upon weather windows, distance from port, vessel requirements, availability of replacement parts and predicted failure rates [56].

The ease of maintenance will be assessed by means of three criteria levels—high, medium and low. High: these devices not only require regular maintenance, but the performance of this maintenance is also difficult. Thus, the maintenance cost is high. Medium: the device requires scheduled maintenance and is moderately easy to access. Low: regular maintenance is required. The performance of the maintenance is also be quite difficult (typically bottom-mounted devices that are difficult to access).

According to [58], an above-waterline WEC with a linear generator PTO, point absorber, and varying depth (more than 50 m) has a medium level of maintenance. The most critical components are underneath the water, making it more complicated to service than floating concepts. For this type of converter, if it is not monitoring, the maintenance can be done only onshore (or on the deck of a vessel).

To conduct an effective EIA study, a crucial element is the environmental monitoring program (EMP), which must establish a system that guarantees the fulfilment of mitigating measures related to the wave energy converters during the entire life process. As is recommended by Riefolo L. et al. [59], future works should include integrating/providing for EIA concerns, performing baseline studies, as well as mitigation measures, monitoring programs and environmental management plans for the entire life processes of wave energy devices.

Modeling is recommended as a method to obtain information about the effects of wave energy on the physical and biological environment, and monitoring is a key component in the development of wave energy projects.

4.2. Economic Aspects of WECs and WPFs

In wave energy, perhaps more so than any other industry, the economics of product development and product ownership are not separate from the product engineering and design. Several economic decision metrics use discounted cash flow, including net present value (NPV) and levelized cost of energy (LCOE). NPV is the most universally applied measure of return of investment across all sectors of investment and LCOE is a widely-used

measure in electricity generation investment (Costello R., et al. [52]). In general terms, LCOE (4.1.) is defined as the ratio of the NPV of total costs over the NPV of all expected electricity production during the project lifetime, defined as [52]:

$$\mathrm{LCOE} = \frac{\sum_{y=0}^{Y} \mathrm{NPV}(\mathrm{CapEx}_y) + \sum_{y=0}^{Y} \mathrm{NPV}(\mathrm{OpEx}_y) + \sum_{y=0}^{Y} \mathrm{NPV}(\mathrm{Dec}_y)}{\sum_{y=0}^{Y} \mathrm{NPV}(\mathrm{AEP}_y)} \quad (13)$$

where LCOE is the levelized cost of electricity [$ or €/kWh], y is year, Y is the lifetime of the project, CapEx is capital expenditure, OpEx is operational expenditure, Dec is decommissioning cost and AEP is annual energy production in kWh.

Due to the fact that WECs are not ommercialized yet capital cost of the WPF is much higher compared to particularly recently well-developed wind and PV power technologies. According to [60] capital costs of WPF varies from 2300 USD/kW on utility (large, power system) scale to over 6200 USD/kW on residential scale, while according to [61] utility scale wind power plants have capital costs of 1500 USD/kW and particularly PV power plants with sharp decrease in last two decades now reached the capital costs of less than 1000 USD/kW on utility scale and from 840–4100 USD/kW depending on the size and country where residential scale is being installed. This sharp decline in capital costs of PV power system is the main reason for authors to assume realistic case scenarios in which WPF will be used together with local residential scale PV system installed by island households themselves. Also, operating costs of WPF is low ranging from 3–4 USD/kWh for utility scale up to 7–10 USD/kWh for residential scale and comparable to one from fossil fuels or wind power plants [60].

According to [60] levelized costs of electricity generation (LCOE) by wave technology range from 8 do 20 EURc/kWh which is significantly higher compared to LCOE of other technologies. For comparison, LCOE of fossil fuels technologies is ranging from 2–10 EURc/kWh depending on technology, but higher LCOE is expected for smaller units appropriate for islands and also distribution of fossil fuels and environmental impact of such technologies are problems to solve. Wind power farms LCOE is ranging from 3–5 EURc/kWh for on-shore to 6–10 EURc/kWh for off-shore but LCOE is strongly related to wind turbine size and island consumption particularly during winter off-season with higher wind potential requires smaller turbines which in turn makes them more expensive and then electricity generation during summer season would not meet the increased consumption. LCOE of PV systems is 6 EURc/kWh in average [60] but even lower LCOE can be expected to to both sharp capital costs decrease and expected high solar radiation in Adriatic/Mediterranean area considered in the paper particularly during summer season high consumption which makes them suitable to be used together with WPF.

Nevertheless, wave energy may compete with other energy sources, as significant reduction in LCOE is expected in the near future, e.g. expected LCOE of 5–7 EURc/KWh beyond 2020 [60]. Also wave energy offers significant benefits over other RES. Wave energy has the highest energy density, minor negative environmental impacts, high predictability andit satisfies electricity demand changes. Power (electricity) extraction from wave energy is continuous for 90% of the day compared to 20% and 30% for wind and solar energy (Fadaeenejad et al.) [62]. This makes the particularly suitable to be used combined with highly variable RES such as wind and solar energy for secure and reliable electricity supply from RES.Wave energy also has social benefits over traditional fossil fuel generation options. These social benefits include providing a new environmentally friendly and easily assimilated grid, avoiding problems that plague so many infrastructure projects; reducing dependence on imported energy supplies and the risk of future fossil fuel price volatility; reducing emissions of greenhouse gases; and promoting local job creation and economic development (Bedard, R.) [63].

5. Discussion

Case study 1 was carried out to determine the optimal number of WECs needed to achieve nearly zero electricity exchange of the LVTF and the upstream network. Case study 2 was performed to point out the advantages and possible problems in operation that can occur when integrating PV systems with this feeder and to alleviate the increase in consumption during the summer period (tourist season). The same situation was studied with winter-period consumption and generation profiles in case study 3, in order to determine the influence of overall electricity generation from both WPF and PV systems during the winter period (off tourist season) as well.

The aim of this study was to achieve net zero exchange of electricity, which was easier to accomplish using PV systems to cover the increased demand during the summer season (tourist season). Electricity generation from wind power plants is very low during the summer in regional climatic conditions. Additionally, wind turbines can be too large for small communities, and additional benefit analysis could be done in the future research to identify the most economical and technically viable energy mix for small island communities.

The presented case studies have a number of limitations. Firstly, an average seasonal sea state was utilized to create a wave time series using a modified JONSWAP spectral function. It was assumed that the sea state remained constant during the whole day. However, the sea state may vary during the season, including completely calm days. More detailed analysis based on the wave power potential available in the Adriatic Sea, correlated with solar irradiation, would help to analyze the energy flow and dimensions of an energy storage more precisely with the goal of maintaining zero power exchange with the grid. Secondly, the power potential was assessed using the third generation wave model Wave Modelling (WAM) for deep sea waves and calibrated with satellite measurements. For the precise assessment of wave potential nearshore, a different prediction model such as Sea Waves Nearshore (SWAN) should be utilized. Thirdly, WECs are usually installed at relatively shallow waters with a depth of up to 100 m. The UU's WEC can safely be installed and operated at 50 m depth. Location L4 has a larger depth, and therefore the WPF should be installed closer to the island shoreline, but then the wave climate would be milder that at L4. Fourthly, offshore installations (e.g., WPF) can face resistance from local communities. Although the UU's WPF has minimal visual impact if located several kilometers offshore, its installation inevitably leads to creating protected areas where fishing and sailing are forbidden. Finally, all presented calculations are influenced by the network element ratings and upstream grid strength (voltage robustness). The calculations were performed for a realistic weak island grid strength; however, in the case of even weaker upstream grid strength, expected particulary on smaller islands, more voltage and power fluctuations as well as exceeding of limits could be expected.

6. Conclusions

The study demonstrated the technical possibility of the integration of a WPF into the low voltage weak grid of an Adriatic island with a typical demand profile which is higher for the summer season. The study showed that a WPF consisting of two WECs is optimal for such a small power grid, and it is effectively complemented by the installation of domestic PVs. The combination of RES with a BESS contributed to the reduction of the intermittency of the power flow, which has a positive effect on the grid and reduces dependency on the grid connection to the mainland. Integration of a larger number of WECs to the same grid leads to the overproduction of electrical power. Finally, the possible deployment of a WPF in combination with PV systems and BESS into a distribution network or microgrids on the coastline of the Adriatic Sea (also applicable to other Mediterranean areas) and particularly on islands, indicated that there are clear benefits to enabling a reliable supply of rapidly increasing electricity demand (consumption) during the tourist season, reaching a net zero grid exchange standard that could play a significant role in faster commercialization of WECs in low energy potential seas.

The optimal number of WECs determined was mainly influenced by the net consumption of the feeder. In the case of the very likely scenario in which the additional generation of electricity is provided by the residential-scale PV systems, concerning problems with voltage regulation and loadability can occur. These possible problems can be mitigated with grid hosting capacity enhancment methods, such as grid reinforcements, network reconfiguration, energy storage devices, OLTCs, reactive power provision, etc. Hovever, as presented in the study, the concept of self-sufficient electricity supply from RES generation is possible, and very likely to be utilized in small-scale islands with wave and solar energy potential.

A BESS used for WPF output power profile smoothing proved to be very efficient with intermittency mitigation. This kind of power-electronic-based device can be utilized in a different manner, such as a community-scale BESS connected at the beginning of the feeder to regulate active and reactive power flows with a reactive power provision to regulate loading and voltages.

Future research should focus on this, as well as on its influence on power quality indices, particulary flickers and harmonic distorsion. Finally, electricity generation by WECs is generally environmentally friendly. It creates new jobs and is economically effective, since operation and maintenance costs are lower for the resource price than when fossil fuels are utilized for energy production. However, economical and life cycle analysis of WPF installation needs to be carried out to see the financial benefits and to estimate the CO_2 reductions for the region.

Author Contributions: Conceptualization, D.Š.; methodology, I.T., M.Ž.; validation, D.Š., I.T., B.N.-S., M.Ž.; formal analysis, I.T., M.Ž.; investigation, D.Š., I.T., B.N.-S.; resources, I.T.; data curation, I.T., M.Ž.; writing—original draft preparation, D.Š., I.T., B.N.-S., M.Ž.; writing—review and editing, D.Š., I.T., B.N.-S., M.Ž.; visualization, I.T., M.Ž.; supervision, B.N.-S. All authors have read and agreed to the published version of the manuscript.

Funding: This article is based upon work from COST Action CA17105 WECANet, supported by COST (European Cooperation in Science and Technology) which is funded by the Horizon 2020 Framework Programme of the European Union. COST is a funding agency for research and innovation networks. COST Actions help connect research initiatives across Europe and enable scientists to grow their ideas by sharing them with their peers. This boosts their research, career and innovation. Irina Temiz would also like to acknowledge financial support from STandUp for Energy, Uppsala University and ÅForsk (PA No. 17550).

Data Availability Statement: Data sharing not applicable.

Conflicts of Interest: The authors declare no conflict of interest. The funders had no role in the design of the study; in the collection, analyses, or interpretation of data; in the writing of the manuscript, or in the decision to publish the results.

References

1. Jäger-Waldau, A. *PV Status Report 2019*; EUR 29938 EN; Publications Office of the European Union: Luxembourg, 2019; ISBN 978-92-76-12608-9.
2. Telsnig, T.; Vazquez, H.C. *Wind Energy: Technology Market Report*; EUR 29922 EN; Publications Office of the European Union: Luxembourg, 2019; ISBN 978-92-76-12569-3.
3. Olauson, J.; Ayob, M.N.; Bergkvist, M.; Carpman, N.; Castellucci, V.; Goude, A.; Lingfors, D.; Waters, R.; Widén, J. Net load variability in Nordic countries with a highly or fully renewable power system. *Nat. Energy* **2016**, *1*, 16175. [CrossRef]
4. Reikard, G.; Robertson, B.; Bidlot, J.R. Combining wave energy with wind and solar: Short-term forecasting. *Renew. Energy* **2015**, *81*, 442–456. [CrossRef]
5. Khan, N.; Kalair, A.; Abas, N.; Haider, A. Review of ocean tidal, wave and thermal energy technologies. *Renew. Sustain. Energy Rev.* **2017**, *72*, 590–604. [CrossRef]
6. Robertson, B.; Hiles, C.; Luczko, E.; Buckham, B. Quantifying wave power and wave energy converter array production potential. *Int. J. Mar. Energy* **2016**, *14*, 143–160. [CrossRef]
7. Waters, R.; Engström, J.; Isberg, J.; Leijon, M. Wave climate off the Swedish west coast. *Renew. Energy* **2009**, *34*, 1600–1606. [CrossRef]
8. Lund, H. Renewable energy strategies for sustainable development. *Energy* **2007**, *32*, 912–919. [CrossRef]
9. *World Energy Council, World Energy Resources 2016*; World Energy Council: London, UK, 2016; ISBN 978 0 946121 29 8.

10. Gunn, K.; Stock-Williansm, C. Quantifying the global wave power resource. *Renew. Energy* **2012**, *44*, 269–304.
11. Vicinanza, D.; Cappietti, L.; Ferrante, V.; Contestabile, P. Estimation of the wave energy in the Italian offshore. *J. Coast. Res.* **2011**, *64*, 613–617.
12. Jakimavičius, D.; Kriaučiūnienė, J.; Šarauskienė, D. Assessment of wave climate and energy resources in the Baltic Sea nearshore (Lithuanian territorial water). *Oceanologia* **2018**, *60*, 207–218. [CrossRef]
13. Alamian, R.; Shafaghat, R.; Miri, S.J.; Yazdanshenas, N.; Shakeri, M. Evaluation of technologies for harvesting wave energy in Caspian Sea. *Renew. Sustain. Energy Rev.* **2014**, *32*, 468–476. [CrossRef]
14. Langodan, S.; Viswanadhapalli, Y.; Dasari, H.P.; Knio, O.; Hoteit, I. A high-resolution assessment of wind and wave energy potentials in the Red Sea. *Appl. Energy* **2016**, *181*, 244–255. [CrossRef]
15. Bozzi, S.; Besio, G.; Passoni, G. Wave power technologies for the Mediterranean offshore: Scaling and performance analysis. *Coast. Eng.* **2018**, *136*, 130–146. [CrossRef]
16. Franzitta, V.; Curto, D.; Milone, D.; Rao, D. Assessment of renewable sources for the energy consumption in Malta in the Mediterranean Sea. *Energies* **2016**, *9*, 1034. [CrossRef]
17. Qiu, S.; Liu, K.; Wang, D.; Ye, J.; Liang, F. A comprehensive review of ocean wave energy research and development in China. *Renew. Sustain. Energy Rev.* **2019**, *113*, 109271. [CrossRef]
18. Contestabile, P.; Lauro, E.D.; Galli, P.; Corselli, C.; Vicinanza, D. Offshore Wind and Wave Energy Assessment around Malè and Magoodhoo Island (Maldives). *Sustainability* **2017**, *9*, 613. [CrossRef]
19. Stojkov, M. Wave energy technologies selection based on comparison in Adriatic Sea by different variable input data and optimal electric connection. In Proceedings of the Wecanet-Wecanet Cost Action CA17105 General Assembly 2019—Book of Abstracts, Porto, Portugal, 28–29 November 2019; p. 82.
20. Farkas, A.; Parunov, J.; Katalinić, M. Wave Statistics for the Middle Adriatic Sea. *J. Marit. Transp. Sci.* **2016**, *52*, 33–47. [CrossRef]
21. Farkas, A.; Degiuli, N.; Martić, I. Assessment of offshore wave energy potential in the croatian part of the Adriatic sea and comparison with wind energy potential. *Energies* **2019**, *12*, 2357. [CrossRef]
22. Katalinić, M.; Ćorak, M.; Parunov, J. Analysis of wave heights and wind speeds in the Adriatic Sea. In Proceedings of the 2nd International Conference on Maritime Technology and Engineering (MARTECH 2014), Lisbon, Portugal, 5–7 October 2014; pp. 1389–1394.
23. Falnes, J. *Ocean Waves and Oscillating Systems: Linear Interactions Including Wave-Energy Extraction*; Cambridge University Press: Cambridge, UK, 2002; ISBN 1139431935.
24. Katalinić, M.; Ćorak, M.; Parunov, J. Optimized wave spectrum definition for the Adriatic Sea. *Nase More* **2020**, *67*, 19–23. [CrossRef]
25. Clément, A.; McCullen, P.; Falcão, A.; Fiorentino, A.; Gardner, F.; Hammarlund, K.; Lemonis, G.; Lewis, T.; Nielsen, K.; Petroncini, S.; et al. Wave energy in Europe: Current status and perspectives. *Renew. Sustain. Energy Rev.* **2002**, *6*, 405–431. [CrossRef]
26. Antonio, F.D.O. Wave energy utilization: A review of the technologies. *Renew. Sustain. Energy Rev.* **2010**, *14*, 899–918.
27. López, I.; Andreu, J.; Ceballos, S.; Martínez De Alegría, I.; Kortabarria, I. Review of wave energy technologies and the necessary power-equipment. *Renew. Sustain. Energy Rev.* **2013**, *27*, 413–434. [CrossRef]
28. Waters, R.; Stålberg, M.; Danielsson, O.; Svensson, O.; Gustafsson, S.; Strömstedt, E.; Eriksson, M.; Sundberg, J.; Leijon, M. Experimental results from sea trials of an offshore wave energy system. *Appl. Phys. Lett.* **2007**, *90*, 034105. [CrossRef]
29. Thorburn, K.; Leijon, M. Farm size comparison with analytical model of linear generator wave energy converters. *Ocean Eng.* **2007**, *34*, 908–916. [CrossRef]
30. Lejerskog, E.; Gravråkmo, H.; Savin, A.; Strömstedt, E.; Tyrberg, S.; Haikonen, K.; Boström, C.; Rahman, M.; Ekström, R.; Svensson, O.; et al. Lysekil Research Site, Sweden: A Status Update. In Proceedings of the the 9th European Wave and Tidal Energy Conference, Southampton, UK, 5–9 September 2011.
31. Anttila, S.; Cardoso, D.; Temiz, I.; Oliveira, J.G.; Leijon, J.; Parwal, A.; Boström, C. Power control strategies for a smoother power output from a wave power plant. In Proceedings of the 13th European Wave and Tidal Energy Conference (EWTEC), Napoli, Italy, 1–6 September 2019; pp. 1–7.
32. Temiz, I.; Leijon, J.; Ekergård, B.; Boström, C. Economic aspects of latching control for a wave energy converter with a direct drive linear generator power take-off. *Renew. Energy* **2018**, *128*, 57–67. [CrossRef]
33. Eriksson, M.; Waters, R.; Svensson, O.; Isberg, J.; Leijon, M. Wave power absorption: Experiments in open sea and simulation. *J. Appl. Phys.* **2007**, *102*, 084910. [CrossRef]
34. Hong, Y.; Eriksson, M.; Castellucci, V.; Boström, C.; Waters, R. Linear generator-based wave energy converter model with experimental verification and three loading strategies. *IET Renew. Power Gener.* **2015**, *10*, 349–359. [CrossRef]
35. Hultman, E.; Ekergård, B.; Kamf, T.; Salar, D.; Leijon, M. Preparing the Uppsala University Wave Energy Converter Generator for Large-Scale Production. In Proceedings of the 5th International Conference on Ocean Energy, Halifax, Canada, 4–6 November 2014; pp. 4–6.
36. Kurupath, V.; Ekström, R.; Leijon, M. Optimal constant dc link voltage operation of awave energy converter. *Energies* **2013**, *6*, 1993–2006. [CrossRef]
37. Bollen, M.H.J.; Hassan, F. *Integration of Distributed Generation in the Power System*; IEEE Press Series on Power Engineering; Wiley: Hoboken, NJ, USA, 2011; ISBN 9780470643372.

38. Znidarec, M.; Sljivac, D.; Topic, D. Influence of distributed generation from renewable energy sources on distribution network hosting capacity. In Proceedings of the 2017 6th International Youth Conference on Energy (IYCE), Budapest, Hungary, 21–24 June 2017; pp. 1–7.
39. Du Bois, A.; De Jaeger, E.; Martin, B. Hosting capacity of LV distribution grids for small distributed generation units, referring to voltage level and unbalance. In Proceedings of the 22nd International Conference and Exhibition on Electricity Distribution (CIRED 2013), Stockholm, Sweden, 10–13 June 2013; Institution of Engineering and Technology: London, UK, 2013; p. 1303.
40. Falabretti, D.; Merlo, M.; Delfanti, M. Network Reconfiguration and Storage Systems for the Hosting Capacity Improvement. In Proceedings of the 22nd International Conference and Exhibition on Electricity Distribution (CIRED 2013), Stockholm, Sweden, 10–13 June 2013; Institution of Engineering and Technology: London, UK, 2013; p. 1504.
41. Meuser, M.; Vennegeerts, H.; Schäfer, P. Impact of voltage control by distributed generation on hosting capacity and reactive power balance in distribution grids. In Proceedings of the CIRED 2012 Workshop: Integration of Renewables into the Distribution Grid, Lisbon, Portugal, 29–30 May 2012; IET: London, UK, 2012; p. 87.
42. Wieland, T.; Otto, F.; Fickert, L. Impact and analysis of different source- and load-characteristics on the feed-in capacity of decentralized generation units in the distribution grid. In Proceedings of the 2013 4th International Youth Conference on Energy (IYCE), Siófok, Hungary, 6–8 June 2013; pp. 1–6.
43. Capitanescu, F.; Ochoa, L.F.; Margossian, H.; Hatziargyriou, N.D. Assessing the Potential of Network Reconfiguration to Improve Distributed Generation Hosting Capacity in Active Distribution Systems. *IEEE Trans. Power Syst.* **2015**, *30*, 346–356. [CrossRef]
44. Wang, S.; Chen, S.; Ge, L.; Wu, L. Distributed Generation Hosting Capacity Evaluation for Distribution Systems Considering the Robust Optimal Operation of OLTC and SVC. *IEEE Trans. Sustain. Energy* **2016**, *7*, 1111–1123. [CrossRef]
45. IEEE The IEEE European Low Voltage Test Feeder. Available online: https://site.ieee.org/pes-testfeeders/resources/ (accessed on 6 November 2020).
46. Electric Power Research Institute OpenDSS, Distribution System Simulator. Available online: http://sourceforge.net/projects/electricdss (accessed on 6 November 2020).
47. European Commission JRC Photovoltaic Geographical Information System (PVGIS). Available online: https://ec.europa.eu/jrc/en/pvgis (accessed on 22 June 2020).
48. Copping, A. *The State of Knowledge for Environmental Effects: Driving Consenting/Permitting for the Marine Renewable Energy Industry*; Pacific Northwest National Laboratory (PNNL), Ocean Energy Systems (OES): Lisbon, Portugal, 2018.
49. Boehlert, G.; McMurray, G.; Tortorici, C.; Klure, J.; Meyer, J. *Ecological Effects of Wave Energy Development in the Pacific Northwest*; US Department Commerce, National Oceanic and Atmospheric Administration (NOAA): Newport, OR, USA, 2008.
50. Greaves, D.; Conley, D.; Magagna, D.; Aires, E.; Chambel Leitão, J.; Witt, M.; Embling, C.B.; Godley, B.J.; Bicknell, A.W.J.; Saulnier, J.-B.; et al. Environmental Impact Assessment: Gathering experiences from wave energy test centres in Europe. *Int. J. Mar. Energy* **2016**, *14*, 68–79. [CrossRef]
51. Chen, Z.; Yu, H.; Hu, M.; Meng, G.; Wen, C. A Review of Offshore Wave Energy Extraction System. *Adv. Mech. Eng.* **2013**, *5*, 623020. [CrossRef]
52. Beyene, A.; Wilson, J.; Garoma, T.; Stiber, B. *Environmental Impact Assessment Tool for Wave Energy Conversion*; San Diego State University, California Energy Commision: Sacramento, CA, USA, 2015.
53. Uihlein, A.; Magagna, D. Wave and tidal current energy—A review of the current state of research beyond technology. *Renew. Sustain. Energy Rev.* **2016**, *58*, 1070–1081. [CrossRef]
54. Roberts, J.D.; Al, E. An environmental impact assessment framework for wave energy installations. In Proceedings of the 5th Annual Marine Energy Technology Symposium (METS), Washington, DC, USA, 1–3 May 2017.
55. Margheritini, L.; Hansen, A.M.; Frigaard, P. A method for EIA scoping of wave energy converters—Based on classification of the used technology. *Environ. Impact Assess. Rev.* **2012**, *32*, 33–44. [CrossRef]
56. Ochs, M.E.; Bull, D.L.; Laird, D.L.; Jepsen, R.A.; Boren, B. *Technological Cost-Reduction Pathways for Point Absorber Wave Energy Converters in the Marine Hydrokinetic Environment*; Sandia National Laboratories: Albuquerque, NM, USA; Livermore, CA, USA, 2013.
57. Kolios, A.; Di Maio, L.F.; Wang, L.; Cui, L.; Sheng, Q. Reliability assessment of point-absorber wave energy converters. *Ocean Eng.* **2018**, *163*, 40–50. [CrossRef]
58. Joubert, J.R.; van Niekerk, J.L.; Reinecke, J.; Meyer, I. *Wave Energy Converters (WECs)*; Stellenbosch University: Stellenbosch, South Africa, 2013.
59. Riefolo, L.; Lanfredi, C.; Azzellino, A.; Vicinanza, D. Environmental Impact Assessment of Wave Energy Converters: A Review. In Proceedings of the International Conference on Applied Coastal Research SCACR, Florence, Italy, 28 September–1 October 2015.
60. Erdoğdu, M.M.; Arun, T.; Ahmad, I.H. *Handbook of Research on Green Economic Development Initiatives and Strategies*; Practice, Progress, and Proficiency in Sustainability; IGI Global: Pennsylvania, PA, USA, 2016; ISBN 9781522504405.
61. Taylor, M.; Ralon, P.; Anuta, H.; Al-Zoghoul, S. *IRENA Renewable Power Generation Costs in 2019*; International Renewable Energy Agency: Abu Dhabi, UAE, 2020.
62. Fadaeenejad, M.; Shamsipour, R.; Rokni, S.D.; Gomes, C. New approaches in harnessing wave energy: With special attention to small islands. *Renew. Sustain. Energy Rev.* **2014**, *29*, 345–354. [CrossRef]
63. Bedard, R. Economic and Social Benefits from Wave Energy Conversion Marine Technology. *Mar. Technol. Soc. J.* **2007**, *41*, 44–50. [CrossRef]